Journal of Organometallic Chemistry, 427 (1992) 101–110
Elsevier Sequoia S.A., Lausanne
JOM 22389

The effect of interannular bridge on electron-transfer rate in mixed-valence biferrocenium triiodide salts

Teng-Yuan Dong, Ting-Yu Lee and Hsiu-Mei Lin
Institute of Chemistry, Academia Sinica, Nankang, Taipei (Taiwan, ROC)

(Received August 23, 1991)

Abstract

The physical properties of the new mixed-valence 1′,3:1‴,3″-bis(propane-1,3-diyl)-1,1″-biferrocenium triiodide (**1**) and 1′,3:1‴,3″-bis(pentane-1,5-diyl)-1,1″-biferrocenium triiodide (**2**) are reported. Compound **1** gives a Mössbauer spectrum with a single "average-valence" doublet at 77 K. On the other hand, compound **2** gives a Mössbauer spectrum with two quadrupole-split doublets at 300 K. Furthermore, compound **1** shows relatively EPR isotropic g tensors compared to compound **2**. Therefore, compound **1** is judged to have an electron-transfer rate in excess of $\sim 10^{10}$ s^{-1}, whereas the electron-transfer rate for **2** is slower than $\sim 10^{7}$ s^{-1}. Both compounds are localized on the IR timescale. Thus, the change of interannular bridge in biferrocenium cations leads to a dramatic influence on the rate of electron transfer. It is concluded that compound **1** has a higher degree of electronic coupling between two iron ions than compound **2**. This difference in rate possibly originates in a structural difference in the interannular bridge in **1** and **2**.

Introduction

Recently, considerable progress has been made in understanding what factors influence the rate of intramolecular electron transfer in the solid state of mixed-valence cations **3**–**10** (Scheme 1) [1–11]. Compounds **3**–**7** give unusual temperature-dependent Mössbauer spectra [2–5]. At temperatures below 200 K they each show two doublets, one for the Fe^{II} and the other for the Fe^{III} sites. Increasing the sample temperature in each case causes the two doublets to merge together with no discernible line broadening, eventually to become a single "average-valence" doublet at temperatures of 365, 275, 245, 275 and 260 K, for **3**, **4**, **5**, **6**, and **7**, respectively. However, pronounced dependence of the rate of electron transfer on sample history has been noted for compounds **6** and **7** [4]. It is even more surprising that the cations **8** and **9** show only one doublet in their Mössbauer spectra at a temperature as low as 4.2 K [12]. On the other hand, compound **10** shows two doublets in its 340 K Mössbauer spectrum (electron-transfer rate $< 10^{7}$ s^{-1}). We suggest that the rates of electron transfer in **3**–**10** can be sensitively

Correspondence to: Dr. T.-Y. Dong, Institute of Chemistry, Academia Sinica, Nankang, Taipei, Taiwan ROC.

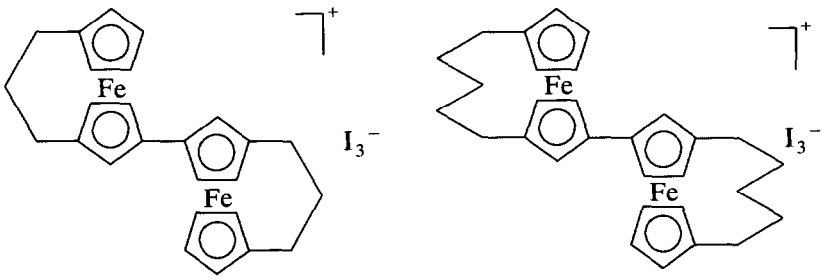

(1) (2)

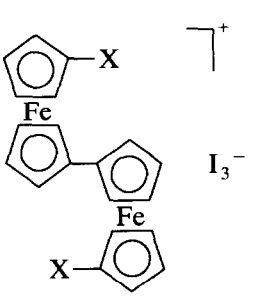

(3) X = H
(4) X = C_2H_5
(5) X = n-C_3H_7
(6) X = n-C_4H_9
(7) X = $CH_2C_6H_5$
(8) X = I
(9) X = Br
(10) X = Cl

Scheme 1.

controlled by environmental factors. The environmental control of intramolecular electron-transfer rates in the mixed-valence trinuclear iron acetate complexes has also been found in the past [13,14]. Such environmental factors are well known in the case of electron transfer in the solution state, arising from the changes in solvent polarization, and they form the central aspects of the Marcus and related kinetic treatments [15,16].

In spite of considerable work in this area, there are still some important unsolved questions. Does the substitutent on the cyclopentadienyl (Cp) ring play a significant role in the electron transfer? How does the lattice dynamics associate with the electron transfer coordinate? To increase our sparse knowledge in this area, we have prepared the new mixed-valence cations **1** and **2**. It has been reported that the unisolated monocation of **1** [17] prepared by controlled current oxidation shows an intervalence transition band at 5520 cm^{-1} in the solution state. Very recently, we have presented a preliminary report [18] that there is a significant influence on the electron-transfer rate of **1** as the Cp rings tilt. In this paper we report the physical properties of **1** and **2** in the solid state. Furthermore, the unusual physical properties of **3–10** are explained in terms of structural characteristics.

Experimental section

General methods

The general preparation of **1** and **2** is shown in Scheme 2. Compounds of **11**, **12**, and **17** were prepared as described in the literature and identified by melting point, ^1H NMR, and mass spectra [17,19].

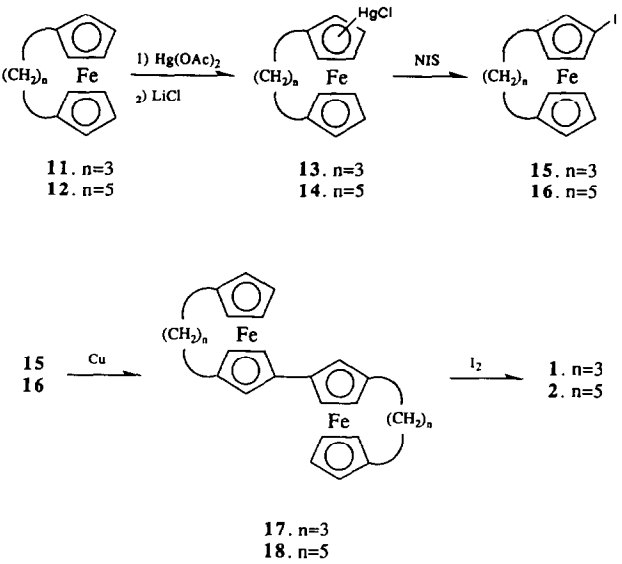

Scheme 2.

Column chromatography was done with the use of neutral alumina (Merk activity I) as the stationary phase. Solvents were purified as follows: benzene, hexane, and ether distilled from Na/benzophenone; CH_2Cl_2 distilled from P_2O_5.

Mercuration of ***12***

The modified procedure described for the synthesis of **13** was used here to prepare **14** [17]. One hundred milliliters of CH_3OH mercuric acetate (14.18 g, 13.1 mmol) was added dropwise to a hot solution of **12** (4.40 g, 17.3 mmol) dissolved in 100 ml of absolute CH_3OH and 65 ml of dry ether. The mixture was refluxed for 6 h, and then LiCl (0.62 g, 14.6 mmol) in 80 ml of hot CH_3OH was added dropwise. A yellow precipitate formed immediately out of an orange solution. The solvent was removed under vacuum. The resulting yellow powder was put into a Soxhlet extractor and extracted with hexane to yield 2.71 g of starting material. Further extraction with CH_2Cl_2 yielded 2.4 g of yellow solid **14**. The crude product could be purified by recrystallization from CH_2Cl_2/hexane.

Iodination of ***14***

The same method described for the preparation of **15** was used to synthesize **16** [17]. The properties of **16** are as follows. ^{1}H NMR ($CDCl_3$) δ 3.5–4.5 (7H, m, ring protons), 1.5–2.5 (10H, m, methylene protons); mass spectrum, M^+/e at 380.

*Neutral 1',3:1''',3''-bis(pentane-1,5-diyl)-1,1''-biferrocene (****18****)*

Compound **18** was prepared by the Ullman coupling procedure for the preparation of **17** [17]. When starting with 0.48 g of **16** and 1 g of activated Cu, hexane extraction yielded 150 mg of the desired biferrocene that was recrystallized from hexane. The properties of **18** are as follows. ^{1}H NMR ($CDCl_3$) δ 3.5–4.5 (14H, m, ring protons), 2.72 (4H, m), 2.32 (8H, m), 1.80 (8H, m, methylene protons); mass spectrum, M^+/e at 506.

Mixed-valence compounds 1 and 2

Samples of **1** and **2** were prepared according to the simple procedure previously reported for **1** [20]. A microcrystalline compound results when a benzene solution of I_2 is slowly added to a benzene solution of the corresponding biferrocene. Anal. **1**: Found: C, 37.62; H, 3.18. $C_{26}H_{26}Fe_2I_3$ calc.: C, 37.58; H, 3.15%. Anal. **2**: Found: C, 40.18; H, 3.53. $C_{30}H_{34}Fe_2I_3$ calc.: C, 40.62; H, 3.86%.

Physical methods

At the Academia Sinica, ^{57}Fe Mössbauer measurements were made on a constant-acceleration-type instrument which has been described previously [21]. Velocity calibrations were obtained with the use of a 99.99% pure 10-μm iron foil. Typical line widths for all three pairs of iron lines fell in the range of 0.25–0.28 mm s^{-1}. Isomer shifts are reported with respect to iron foil at 300 K, but are uncorrected for temperature-dependence.

^1H NMR spectra were run on a Bruker MSL 200 spectrometer. Mass spectra were obtained with a VG system, Model 70-250 S. Electron paramagnetic resonance data (X-band) were collected with a Bruker 200D-SRC spectrometer. The magnetic field was calibrated with a Bruker NMR gauss meter ER035M. DPPH was used to gauge the microwave frequency. A direct-immersion dewar, which was inserted into the cavity, was used to obtain data at 77 K.

Results and discussion

Mössbauer characteristics

Mössbauer spectra were run at 300 and 77 K for compounds **1** and **2**. As shown in Fig. 1 and Table 1, the Mössbauer results indicate that compound **1** is delocalized on the Mössbauer timescale above 77 K. Only a single "average-valence" doublet is seen for **1** at either 300 or 77 K. The value of the quadrupole splitting (ΔE_Q 1.6140 mm s^{-1}) at 77 K could indicate that there is a strong electronic coupling between the *d*-manifolds on the two iron ions in **1**. This does not happen for **3–10** ($\Delta E_Q \sim 1.2$ mm s^{-1}) [2–5,12], but it does occur in the dibridged delocalized mixed-valence cations **19** and **20** (Scheme 3). Both compounds exhibit one quadrupole-split doublet. In the case of **19**, ΔE_Q was reported to be 1.519(5) mm s^{-1} at 300 K [22–24]. The value of ΔE_Q at 300 K for **20** is even larger (1.719(3) mm s^{-1}) [5,24]. Furthermore, we believe that the unusual ΔE_Q in **1** is not contributed from the interannular methylene bridge. When the Cp rings in ferrocene are linked by an interannular bridge, the Cp rings are displaced from their preferred parallel plane arrangement. Under this circumstance, one may expect a change of ^{57}Fe Mössbauer parameters. However, from our Mössbauer studies on 1,1′-(propane-1,3-diyl)ferrocenium cation, the ΔE_Q does not change significantly as the Cp rings tilt. As given in Table 1, the value of ΔE_Q for 1,1′-(propane-1,3-diyl)ferrocenium triiodide is 0.1484 mm s^{-1}. It has been reported that the ferrocenyl groups give spectra characterized by large quadrupole splittings in the range of 2.0–2.5 mm s^{-1}, while the spectra of ferrocenium cations are characterized by a small or vanishing ΔE_Q [20]. The vanishing of ΔE_Q in the ferrocenium cation with respect to ferrocene is mainly due to the decrease in $d_{x^2-y^2}$ and d_{xy} (e_{2g}) population, associated with the removal of one electron from ferrocene. Thus, the interannular bridged ferrocenium cations are consistent with

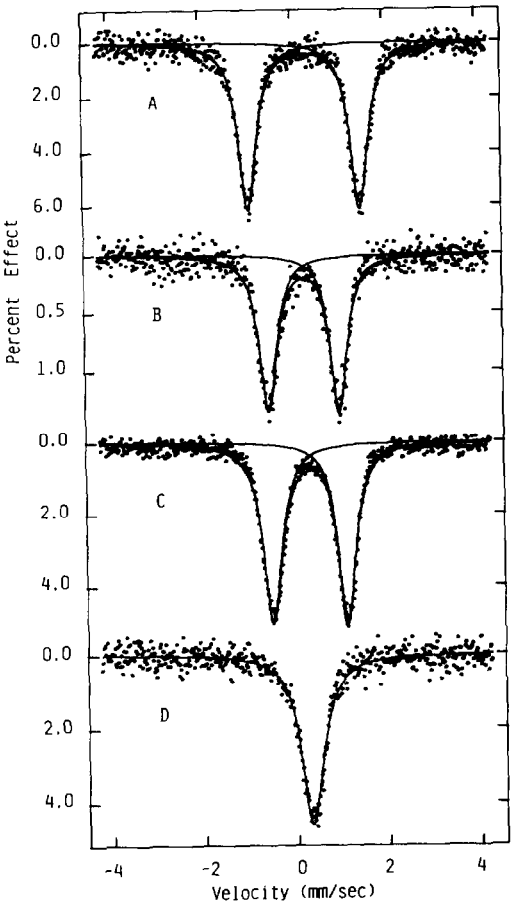

Fig. 1. ^{57}Fe Mössbauer spectra for (A) **17**, (B) **1** at 300 K, (C) **1** at 77 K, and (D) 1,1′-(propane-1,3-diyl)ferrocenium triiodide.

Table 1

^{57}Fe Mössbauer least-squares fitting parameters

Compound	T	ΔE_Q [a]	δ [b]	Γ [c]
1′,3:1‴,3″-Bis(propane-1,3-diyl)-1,1″-biferrocene	300	2.4222	0.3720	0.4629, 0.4676
1,1′-(Propane-1,3-diyl)-ferrocenium I_3^-	300	0.1484	0.3825	0.3140, 0.4721
1,1′-(Pentane-1,5-diyl)-ferrocenium I_3^-	300	0.2647	0.4342	0.3032, 0.3217
1	300	1.5327	0.3182	0.4470, 0.4654
	77	1.6140	0.4073	0.4573, 0.4877
2	300	0.3900	0.4038	0.4814, 0.5953
		2.0078	0.4464	0.5835, 0.5844
	77	0.3069	0.4141	0.3709, 0.4152
		2.2081	0.4005	0.3097, 0.3012

[a] Quadrupole splitting in units of mm s^{-1}. [b] Isomer shift in unit of mm s^{-1}. [c] Full width at half height taken from the least-squares fitting program. The width for the line at more positive velocity is listed first for each doublet.

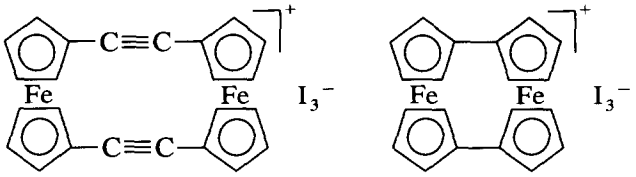

(19) (20)

Scheme 3.

this bonding arrangement. If there was only a weak electronic coupling between two iron ions in **1**, the observed ΔE_Q would approach the average value (1.2853 mm s^{-1}) of ΔE_Q for neutral biferrocene (ΔE_Q 2.4222 mm s^{-1}) and 1,1'-(propane-1,3-diyl)ferrocenium triiodide (ΔE_Q 0.1484 mm s^{-1}). Therefore, the electronic coupling in **1** is strong. There is an appreciable contribution from the fulvenide ligand to the molecular orbital in which the unpaired electron resides. Under this condition, the iron ions lose their Fe^{III} character to some degree, and this loss results in an increase in ΔE_Q because each iron ion is closer to Fe^{II} in its properties.

As illustrated in Fig. 2, the 300 and 77 K Mössbauer spectra of **2** show two doublets, one for the Fe^{II} site and the other for the Fe^{III} site. This pattern of two doublets indicates that the intramolecular electron-transfer rate is less than the Mössbauer timescale ($\sim 10^7$ s^{-1}). Thus, the change from the trimethylene interannular bridge in **1** to the pentamethylene bridge in **2** leads to a dramatic reduction of intramolecular electron-transfer. This change clearly indicates that the interan-

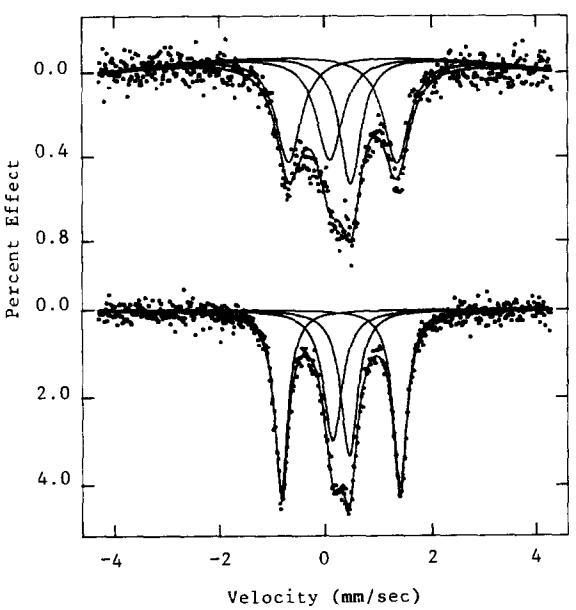

Fig. 2. ^{57}Fe Mössbauer spectra for **2** at 300 K (top) and 77 K (bottom).

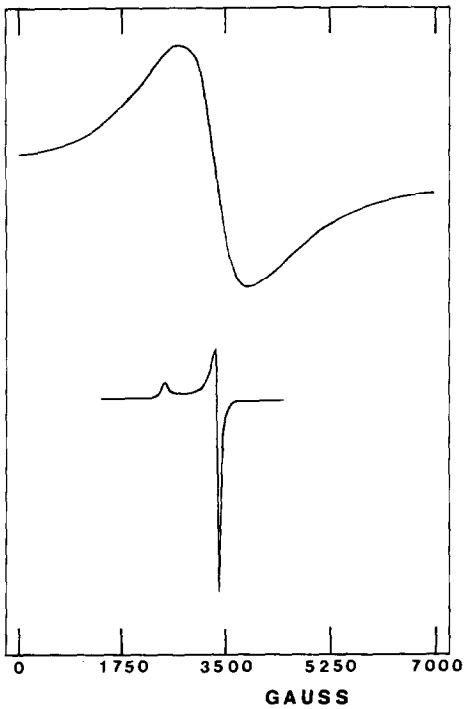

Fig. 3. EPR spectra of **1** at 300 K (top) and 77 K (bottom).

nular bridge plays a crucial role in determining the rate of electron transfer. An explanation for this difference is presented in the last section, which focuses on the different structural characteristics in the mixed-valence biferrocenium cations.

Electron paramagnetic resonance

X-Band EPR spectra were taken at 77 and 300 K for **1**, **2**, and related molecules. An axial-type spectrum was observed at 77 K for **1** and **2**. In the case of **1**, a broad EPR signal is observed at 300 K, as illustrated in Fig. 3. On the other hand, the 300 K EPR spectrum of **2** is silent. The g values extracted from all of these spectra are collected in Table 2, together with some g values for related compounds.

It is interesting that the Δg value for **1** (0.73) suggests that the cation is also delocalized on the EPR timescale (10^9–10^{10} s^{-1}) even at 77 K. In general, there are two diagnoses to tell whether the intramolecular electron-transfer rate in the mixed-valence biferrocenium cation is faster than the EPR timescale. First, the g-tensor anisotropy ($\Delta g = g_{\parallel} - g_{\perp}$) will be less than 0.8, if the rate of electron transfer is faster than the EPR timescale. It has been reported [12] that the value of Δg is considerably reduced for a binuclear mixed-valence biferrocenium cation. Hendrickson suggested that this is a reflection of considerably reduced orbital angular momentum in the ground state which results from admixture of the $S = 0$ Fe^{II} description into the ground state. From Table 2, the Δg value for **1** is 0.73 which is even smaller than that for the delocalized mixed-valence cations **8** and **9**.

Table 2

EPR data for **1**, **2**, and related molecules

Compound	T (K)	$g_{\parallel}$	$g_{\perp}$	Δg [a]
Ferrocenium [b]	20.0	4.35	1.26	3.09
1,1'-(Dimethyl)ferrocenium [b]	12.0	4.00	1.92	2.08
1,1'-(Propane-1,3-diyl)-ferrocenium [c]	77.0	3.75	1.66	2.09
1,1'-(Pentane-1,5-diyl)-ferrocenium [c]	77.0	3.35	1.87	1.48
3 [b]	12.0	3.58	1.72	1.86
4 [b]	3.3	3.02	2.01	1.07
			1.89	
6 [b]	4.2	2.98	1.92	1.06
7 [b]	4.2	3.42	1.84	1.58
8 [b]	4.2	2.75	2.01	0.76
			1.97	
9 [b]	4.2	2.76	2.01	0.78
			1.96	
1 [d]	300.0	2.00		
	77.0	2.71	1.98	0.73
2 [d]	77.0	3.24	1.89	1.35
19 [b]	5.1	2.52	1.97	0.60
			1.88	
20 [b]	12.0	2.36	1.99	0.41
			1.91	

[a] $\Delta g = g_{\parallel} - g_{\perp}$. [b] From ref. 12. [c] In H_2SO_4 frozen solution from ref. 27. [d] This work.

We believe that this is not a reflection of greater low-symmetry crystal field. Prins reported [25] that for a mononuclear Fe^{III} metallocene if there is no low-symmetry crystal field, then $g_{\parallel} = 6$ and $g_{\perp} = 0$. As the low-symmetry crystal field distortion increases, both $g_{\parallel}$ and $g_{\perp}$ approach a value of 2. From the EPR studies of 1,1'-dimethylferrocenium [26] and 1,1'-(propane-1,3-diyl)ferrocenium cations, we suggest that the cation **1** would not experience a greater low-symmetry crystal field than disubstituted biferrocenium cations **4–10**. From Table 2 it can be seen that 1,1'-(propane-1,3-diyl)ferrocenium cation gives an axial 77 K EPR signal characterized by $g_{\parallel} = 3.75$ and $g_{\perp} = 1.66$. The g-tensor anisotropy is 2.09 which is not significantly different from the value of 2.08 for 1,1'-dimethylferrocenium cation. Additional evidence that **1** is delocalized on the EPR timescale is available from the EPR studies of **2**. Compound **2** gives an axial-type EPR spectrum at 77 K ($g_{\parallel} = 3.24$ and $g_{\perp} = 1.89$). The Δg is 1.35 which is quite greater than 0.73 for **1**. In fact, the interannular pentamethylene bridge can contribute a larger low-symmetry crystal field than the trimethylene bridge [27]. The low-symmetry crystal field parameters calculated from the equations given by Prins [25] are 460 and 1000 cm^{-1} for 1,1'-(propane-1,3-diyl)ferrocenium and 1,1'-(pentane-1,5-diyl)ferrocenium cations, respectively. Furthermore, the X-ray structure of 1,1'-(pentane-1,5-diyl)ferrocenium triiodide shows an average ring tilt of 10.8° [27].

Finally, the EPR signals can be readily seen at room temperature, if the electron-transfer rate is delocalized on the EPR timescale. This is also the case for the delocalized molecules **1**, **19** [15,16], and **20** [15]. On the other hand, compound **2** shows a localized electronic structure on the EPR timescale, and it is EPR silent at room temperature.

Infrared spectroscopy

If compound **1** is delocalized on the ^{57}Fe Mössbauer and EPR timescales, the next question is whether the electron-transfer rate is faster than the IR timescale. When Fe^{II} metallocene is oxidized to Fe^{III} metallocene, there is a dramatic change in the IR spectrum. It has been shown [20] that the perpendicular C–H bending band is the best diagnosis of the oxidation state. This band is seen at 815 cm^{-1} for ferrocene and at 850 cm^{-1} for ferrocenium triiodide. The mixed-valence biferrocenium cation which is localized on the IR timescale should exhibit one C–H bending band for the Fe^{II} moiety and one for Fe^{III} moiety. The perpendicular C–H bending bands for **1** are at 818 and 849 cm^{-1}. It is clear that the IR data of **1** conclusively indicate the presence of Fe^{II} and Fe^{III} moieties. In other words, the rate of electron transfer in **1** is less than $\sim 10^{12}$ s^{-1}.

Conclusion

The physical properties of **1** clearly indicate that the intramolecular electron-transfer rate is greater than $\sim 10^9$–10^{10} s^{-1} at 77 K, whereas the rate of electron transfer in **2** is less than $\sim 10^7$ s^{-1} at 300 K. In the solution state, it has been concluded that the unisolated monocation of **1** has a higher degree of electronic coupling between two iron ions than the biferrocenium cation. This difference in rate possibly originates in a structural difference in interannular bridges in **1** and **2**.

The electronic ground state of ferrocene is a singlet. $^1A_{1g}$ ($e_{2g}^4 a_{1g}^2$), where the one-electron molecular orbitals are predominantly *d* orbitals in character: a_{1g} (d_{z^2}) and e_{2g} ($d_{x^2-y^2}$, d_{xy}) [26]. As indicated by magnetic susceptibility [28] and EPR measurements [25], the electronic ground state of ferrocenium is doublet $^2E_{2g}$ ($a_{1g}^2 e_{2g}^3$). In **1** the Cp rings are tilted from the parallel geometry for ferrocene. Lauher and Hoffmann have derived the fragement orbitals for a bent $(Cp)_2M$ unit from the parallel geometry [29]. Bending back the Cp rings splits the e_{2g} set into orbitals of a_1 ($d_{x^2-y^2}$) and b_2 (d_{xy}) symmetry. The a_{1g} orbitals rise rapidly in energy as the Cp rings are bent back. In this case, some metal x^2-y^2 character from a_1 mixes into a_1 which was a_{1g}. This also occurs for 1,1′-(propane-1,3-diyl)ferrocenium cation [27]. The greater the admixture, the greater the probability for unpaired electron density on the a_{1g}. This results in an increase in electronic coupling between two iron ions, and this is what we observe for compound **1**. Furthermore, it appears that there is a correlation between the tilt angle and the rate of electron transfer: the larger the tilt angle, the faster the electron transfer. The tilt angles in each ferrocenyl unit for **3** [4], **4** [30], **5** [31], **7** [32], and **8** [12] are 0.3, 4.7, 6.6, 2.3, and 15.6°, respectively. The transition temperatures from localized to delocalized states on the Mössbauer timescale for **3**, **4**, **5**, and **7** are 365, 275, 245, and 260 K, respectively [4]. Compound **8** is even delocalized at 4.2 K [12]. From this comparison, there is a correlation between the tilt angle and the electron transfer rate, except compound **7**. The rates of electron transfer in the series of **3**–**10** can be sensitively controlled by environmental factors, i.e., the crystal packing arrangement and intermolecular interactions. For instance, the rates of electron transfer in **3**–**10** can be changed by replacing the counterion [33,34]. Hence, the importance of intermolecular interactions in determining the electron-transfer rates in **1**–**10** cannot be excluded, but we propose that the tilting of the Cp rings is an another important factor. Theoretical explanations of the

various factors about intramolecular electron transfer of biferrocenium cations were mostly based on a PKS vibronic model [35] where the magnitude of the vibronic coupling plays an essential role. Taking into account the lattice dynamics, a micromodulation mechanism was proposed [11] to describe the electron transfer assisted by the collective motion which was composed of the local breathing mode of each monomer unit. Obviously, the collective breathing mode could not lead to net tilting. Coupling of the bending mode to the original micromodulating mechanism needs to be closely investigated.

Acknowledgement

We are grateful for support from the ROC National Science Council.

References

1 D.N. Hendrickson, S.M. Oh, T.-Y. Dong, T. Kambara, M.J. Cohn and M.F. Moore, Comments Inorg. Chem., 4 (1985) 329.
2 T.-Y. Dong, M.J. Cohn, D.N. Hendrickson and C.G. Pierpont, J. Am. Chem. Soc., 107 (1985) 4777.
3 M.J. Cohn, T.-Y. Dong, D.N. Hendrickson, S.J. Geib and A.L. Rheingold, J. Chem. Soc., Chem. Commun., (1985) 1095.
4 T.-Y. Dong, D.N. Hendrickson, K. Iwai, M.J. Cohn, S.J. Geib, A.L. Rheingold, H. Sano, I. Motoyama and S. Nakashima, J. Am. Chem. Soc., 107 (1985) 7996.
5 S. Iijima, R. Saida, I. Motoyama and H. Sano, Bull. Chem. Soc., Jpn., 54 (1981) 1375.
6 S. Nakashima, Y. Masuda, I. Motoyama and H. Sano, Bull. Chem. Soc. Jpn., 60 (1987) 1673.
7 S. Nakashima, M. Katada, I. Motoyama and H. Sano, Bull. Chem. Soc. Jpn., 60 (1987) 2253.
8 T.-Y. Dong, T. Kambara and D.N. Hendrickson, J. Am. Chem. Soc., 108 (1986) 4423.
9 T.-Y. Dong, T. Kambara and D.N. Hendrickson, J. Am. Chem. Soc., 108 (1986) 5857.
10 M. Sorai, A. Nishimori, D.N. Hendrickson, T.-Y. Dong and M.J. Cohn, J. Am. Chem. Soc., 109 (1987) 4266.
11 T. Kambara, D.N. Hendrickson, T.-Y. Dong and M.J. Cohn, J. Chem. Phys., 86 (1987) 2326.
12 T.-Y. Dong, D.N. Hendrickson, C.G. Pierpont and M.F. Moore, J. Am. Chem. Soc., 108 (1986) 963.
13 H.G. Jang, S.J. Geib, Y. Kaneko, M. Nakano, M. Sorai, A.L. Rheingold, B. Montez and D.N. Hendrickson, J. Am. Chem. Soc., 111 (1989) 173.
14 Y. Kaneko, M. Nakano, M. Sorai, H.G. Jang and D.N. Hendrickson, Inorg. Chem., 28 (1989) 1067.
15 R.A. Marcus, J. Chem. Phys., 24 (1956) 966.
16 R.A. Marcus, J. Chem. Phys., 43 (1965) 679.
17 D.R. Talham and D.O. Cowan, Organometallics, 6 (1987) 932.
18 T.-Y. Dong and C.Y. Chou, J. Chem. Soc., Chem. Commun., (1990) 1332.
19 T.H. Barr and W.E. Watts, Tetrahedron, 24 (1968) 3219.
20 W.H. Jr. Morrison and D.N. Hendrickson, Inorg. Chem., 14 (1975) 2331.
21 T.-Y. Dong, M.Y. Hwang, T.L. Hsu, C.C. Schei and S.K. Yeh, Inorg. Chem., 29 (1990) 80.
22 C. Levanda, K. Bechgaard and D.O., Cowan, J. Org. Chem., 41 (1976) 2700.
23 J. Kramer and D.N. Hendrickson, Inorg. Chem., 19 (1980) 3330.
24 I. Motoyama, M. Watanabe and H. Sano, Chem. Lett., (1978) 513.
25 R. Prins and A. Kortberk, J. Organomet. Chem., 33 (1971) c33.
26 D.M. Duggan and D.N. Hendrickson, Inorg. Chem., 14 (1975) 95.
27 T.-Y. Dong, H.M. Lin, M.Y. Hwang, T.Y. Lee, S.M. Peng and G.H. Lee, J. Organomet. Chem., 414 (1991) 227.
28 D.N. Hendrickson, Y.S. Sohn and H.B. Gray, Inorg. Chem., 10 (1971) 1559.
29 J.W. Lauher and R. Hoffmann, J. Am. Chem. Soc., 98 (1976) 1729.
30 M. Konno and H. Sano, Bull. Chem. Soc. Jpn., 61 (1988) 1455.
31 M. Konno, S. Hyodo and Iijima, Bull. Chem. Soc. Jpn., 55 (1982) 2327.
32 R.J. Webb, T.-Y. Dong, C.G. Pierpont, S.R. Boone, R.K. Chadha and D.N. Hendrickson, J. Am. Chem. Soc., 113 (1991) 4806.
33 M. Kai, M. Katada and H. Sano, Chem. Lett., (1988) 1523.
34 T.-Y. Dong, C.C. Schei, T.L. Hsu, S.L. Lee and S.J. Li, Inorg. Chem., 30 (1991) 2457.
35 K.Y. Wong and P.N. Schatz, Prog. Inorg. Chem., 28 (1981) 369.